Application of in-trap α spectroscopy to lifetime measurements with MLLTRAP

P. Chauveau[a,*], S. Franchoo[b], K. Hauschild[a], J. Ljungvall[a], A. Lopez-Martens[a], D. Lunney[a], M. MacCormick[b], E. Minaya Ramirez[b], P.G. Thirolf[c], C. Weber[c]

[a] Centre de Sciences Nucléaires et de Sciences de la Matière (CSNSM), CNRS/IN2P3 et Université Paris Sud 11, UMR 8609, 91405 Orsay Campus, France
[b] Institut de Physique Nucléaire d'Orsay, CNRS/IN2P3 et Université Paris Sud 11, UMR 8608, 91406 Orsay Campus, France
[c] Faculty of Physics, Ludwig-Maximilians University Munich, Am Coulombwall 1, D-85748 Garching, Germany

ARTICLE INFO

ABSTRACT

MLLTRAP is a double Penning-trap designed for high precision mass measurements of exotic nuclei. It was built and commissioned off-line at the Maier-Leibnitz Laboratory (MLL) in Garching and is currently installed at the ALTO facility at IPNO, awaiting online commissioning. A complementary double-trap assembly dedicated to in-trap decay spectroscopy is being studied, in which the central electrode of the second trap has been replaced by an arrangement of four silicon-strip detectors (SSD) set at the trapping potential. By using the well-known buffer-gas cooling technique in the first trap we will be able to deliver a spot-like ion cloud of high purity to the detector trap. The decay products being emitted in-flight and not from an implantation material, we expect to achieve high-resolution decay spectroscopy of the confined ion bunch. In the case of heavy α emitters, α particles can be detected by the in-trap SSD, while conversion electrons are guided very efficiently by the magnetic field to another detector, thus allowing for unperturbed detection of both. In addition, once coupled with a position-sensitive electron detector, this spectroscopic trap will allow for indirect measurements of excited-state lifetimes in the region of heavy and super-heavy nuclei, via a new recoil distance measurement method.

1. Introduction

As new and more exotic nuclei were discovered, the need to produce and study them has boosted technical developments in accelerator science and detection systems. The introduction of electromagnetic ion traps was a breakthrough for both, as it enabled the creation and study of ion bunches. The success of ion traps in nuclear physics is due to two main reasons: the trajectories of ions in a trap depend on the mass-to-charge ratio m/q and the ions are maintained in a confined space for extended periods of time. The first enables the separation of ions with respect to their mass or charge state and mass measurement, while the second allows for cooling, storage, high m/q resolving power, and in-trap decay and laser spectroscopy techniques. The instrument described in this paper will take advantage of most of these features.

MLLTRAP is a double Penning trap housed in a 7 T superconducting solenoid. The magnet generates two regions of high field homogeneity at the positions of the first trap (<1.285 ppm) and second trap (<0.285 ppm) [1]. It was built at the Maier-Leibnitz Laboratory (MLL) in Garching, Germany and is currently installed at ALTO in Orsay, France. Ultimately, it will be installed in the upcoming DESIR facility at

SIPRAL2-GANIL in Caen, where it will receive intense proton-rich or super-heavy ion beams from S3 [2]. MLLTRAP was initially designed for high-precision mass measurement and achieved a relative mass uncertainty of 2.9 10^{-8} during its offline tests at MLL [3]. The trap is currently being prepared for online commissioning at ALTO, where the clean laser-ionised photofission beams will allow for mass measurements of fission fragments with lower contamination than at other facilities. MLLTRAP will probe nuclear masses on the neutron-rich side of the valley of stability around neutron shell-closures $N = 50$ and $N = 82$, as these are regions of high astrophysical interest [1]. As with most other double Penning trap systems [4–9], the first trap will center the ions of interest via sideband cooling [10] and the second will measure masses with the ToF-ICR [11] or PI-ICR [12] technique.

A second double-trap assembly is being developed for MLLTRAP, in which the first trap, identical to the one of the first assembly, will still be used for mass-selective centering, while the second trap has been replaced by an arrangement of four SSDs (see Fig. 1), further described in [13–15]. In Penning traps, ion confinement is ensured by the superposition of a uniform magnetic field and an electrostatic field shaped by several electrodes. In the second trap, the voltage bias applied to the
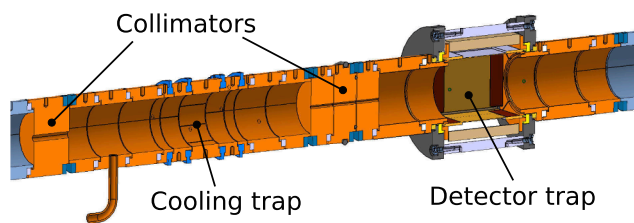

Fig. 1. Mechanical rendering of the spectroscopic double-trap assembly done by the design office at CSNSM. The first trap (left) is cyclindrical with a central segmented electrode. The four silicon detectors (gold) form the second trap (right). The inlet tube located after the first collimator is used for buffer gas injection.

silicon detectors also defines the axial potential well. Such a detector trap system can simultaneously confine a radioactive ion and detect its decay products. The combination of both traps will be particularly suited for the spectroscopy of α-emitting nuclei. The first trap will clean the incoming ion bunch from unwanted contaminants. In the second trap the bunch is an ideal decay source, being essentially pure and free from scattering effects that would arise if the bunch were implanted instead. In addition, electrons below $\simeq 10$ MeV are very efficiently guided along the magnetic field lines towards the fringe field region, meaning that α particles and all subsequently emitted electrons (shake-off, internal conversion, Auger, Coster-Kronig) are separated, allowing for unperturbed detection of both: α particles inside the detector trap and electrons in a separate detector placed within the fringe field. As described in [15], if coupled to a position-sensitive electron detector, this setup opens the path to a new lifetime determination method by Decay and Recoil Imaging (DARING). In this paper we review the progress made on this novel spectroscopic double-trap. After recalling the physics goals of this trap, the final design will be described and simulations of the trap operation and of the DARING method, estimating the trap's capabilities, will be presented.

2. Objectives of the spectroscopic trap

In-trap decay spectroscopy is not yet widespread, but its feasibility was demonstrated by Weissman et al. [16] and some dedicated systems have already been used to detect conversion electrons [17], β particles and protons [18], and even X-rays [19,20]. However, the Larmor radius of decay α particles inside a 5–10 T magnetic field is too large to be guided along the field lines, but also too small to be reliably detected through a window inside the magnet. The novelty of this trap is to use silicon electrodes that fulfill both the roles of detector and trap, the close proximity to the trapping point ensuring a high geometric efficiency of detection. The double-trap system will provide a contamination-free sample, confined but not implanted, allowing for high resolution α spectroscopy. Knowledge of α energies and intensities will give access to basic structure information in the daughter nucleus. The lifetime-measurement method presented here will concern mainly low-lying 2^+ and first excited 0^+ states in heavy to superheavy even-even nuclei. Since these states decay primarily (or exclusively in the 0^+ case) by internal conversion, their lifetime cannot be measured with standard methods involving γ-ray detectors such as fast-timing [21] or plunger [22] techniques. From the lifetime of the 2^+ state, one can derive the corresponding electric quadrupole moment, giving insight on the nuclear deformation. Also, knowing the lifetime of a low-lying 0^+ state will allow to quantify the shape-mixing between this state and the ground state.

3. Mechanical design

Fig. 1 shows the mechanical design of the double trap, which is largely based on the mass measurement assembly presented in [3],

itself based on the cooler trap of ISOLTRAP [5]. All trap electrodes facing the ions (except the silicon detectors) will be made of gold-plated oxygen-free copper in order to preserve the high field homogeneity produced by the superconducting magnet, and will be separated from one another by ceramic insulators. The central electrode of the first trap is segmented eightfold to allow for both quadrupole and octupole excitations. Because of the helium-gas used for the cooling, this trap is isolated from the rest of the assembly by two collimators with 4 mm and 2 mm apertures at the entrance and exit sides, respectively. These collimators mainly protect the second trap for which the gas pressure should be typically below 10^{-8} mbar to avoid ion-gas interactions. In the second trap, the SSDs are fixed to two side-rings via tenon joints. These rings are segmented fourfold to enable the manipulation of eigenmotions inside the second trap and thus mass measurements. For this purpose, the size of the subsequent side-electrodes have been chosen to minimize the field imperfections. The feasibility and precision of mass measurements with the detector trap are still being investigated and will not be discussed in this paper.

4. Trap operation

In-trap α-decay studies can strongly benefit from a purification stage eliminating unwanted by-products of fusion-evaporation reactions. Also, a cooled ion bunch behaves like a point-like source, which reduces the uncertainty of the DARING technique in the detector trap (see next section). The sideband cooling technique has been simulated with SIMION 8.1 [23]. In simulations, the ion-gas interaction was modelled by viscous damping with a helium buffer gas pressure of 10^{-4} mbar. First, a 20 ms, 200 mV dipolar pulse is applied at the magnetron frequency. The pulse being short and the magnetron frequency depending little on the mass, all ions of interest and contaminants are excited. A 255 ms, 45 mV quadrupole excitation at the cyclotron frequency is then applied and converts the magnetron motion into the modified-cyclotron motion. This conversion is mass selective and as the magnetron motion decreases for ions of appropriate mass, their cyclotron motion is continuously damped by the buffer gas, leading to a mass-selective centering. In simulations, the size of a realistic 1 mm wide bunch is reduced by a factor $\simeq 20$, which is consistent with theoretical predictions given in [11]. Though the resolving power of this method can be quite high in theory, the actual separation power of this method also depends on the size of the aperture of the collimator, as ions which are not sufficiently re-centered will be lost on the electrode upon extraction. The separation power for super-heavy masses can be reasonably extrapolated from those measured during the commissioning of the mass-measurement trap [3] to at mass 250.

In perfect vacuum there is no limit to the trapping time and one could confine an ion until it decays. In our case the gas leakage from the first trap limits the time spent by ions inside the second trap without encountering neutral contaminants with which charge exchange could occur. The mean free path associated with each eigenmotion is directly proportional to the amplitude of the said motion. In storage mode, the ions will be close to the center ($\simeq 0.1$ mm radial motions, $\simeq 1$ mm axial motion) allowing to trap ions for several seconds. Active damping of the residual motions with dipolar excitations could also reduce the mean free path per cycle, theoretically allowing to trap ions for over 10 s under a $\simeq 10^{-8}$ mbar pressure. However, since the decay probability does not depend on the elapsed time, it is interesting to frequently re-load the trap with a "fresh" bunch of decaying ions while dumping the old one, even taking into account the small time intervals when the trap is empty in between ejection and injection. Thus it makes sense to use short trapping times below 1 s, like the ones typically required for high precision mass measurements. Because an α-decaying nucleus is lost for mass measurement, whether the α particle is detected or not, this setup could be used simultaneously for α spectroscopy and mass measurement.
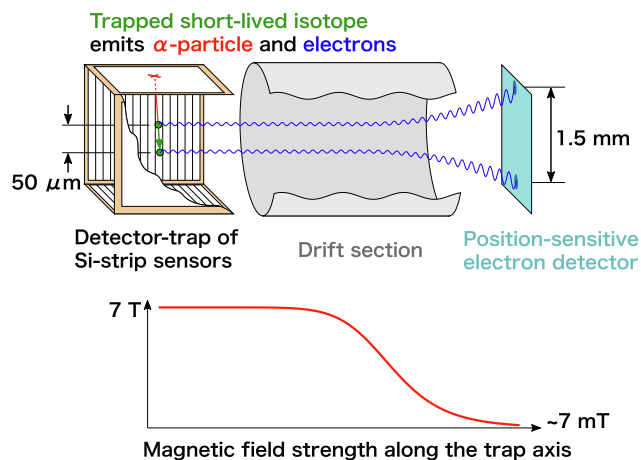
Fig. 2. Principle of DARING. The small distance between electron clouds is magnified in the fringe field to a measurable value. The positions of the clouds on the electron detector and the position of the α particle on the SSD give the geometry of the decay, while the α decay energy allows to deduce the velocity of the recoil.

5. Lifetime measurement

The principle of the DARING method is illustrated in Fig. 2. During α decay, the change of central Coulomb potential shifts the energy of electronic levels and results in the emission of a few shell-rearrangement shake-off electrons. High-energy shake-off electrons may also be emitted following direct collision with the escaping α particle. When the α decay populates a low-lying excited state of the daughter, decay by internal conversion is favored. The vacancy left in the inner electron shells then results in the emission of X-rays and Auger/Coster-Kronig electrons. Thus two electron clouds are emitted marking the time of population and decay of the excited state of the recoiling daughter nucleus. Since this method relies on the excited state decaying via internal conversion, it follows that it can also be applied to measure the half-life of first excited 0+ states. Following α decay, the daughter nucleus recoils, resulting in the two electron emission points being distinct, separated by $\simeq 50\,\mu m$ (for $A = 250$, $T_\alpha = 8\,\mathrm{MeV}$ and $t_{1/2} = 100\,\mathrm{ps}$). The magnetic field then guides the electrons towards a position-sensitive detector located in the fringe field, in which the distance between the clouds is magnified. Information from the electron detector and the in-trap Si-strip detectors then allows to reconstruct the full kinematics of the α decay and the lifetime of the state can be deduced. Possible electron detectors have already been discussed in previous papers [13–15]. However, we introduce here the possibility of using a delay-line anode Micro-Channel Plate (MCP). This detector will already be used to measure the cyclotron frequency of the ions of interest with the PI-ICR method in the mass measurement assembly, and keeping the same post-trap detection system would be an operational advantage. The MCP bias can be changed to allow for high-efficiency electron detection. In addition, this detector would be compatible with low-energy electrons, meaning that little to no post-acceleration would be necessary as it would be the case with Si-based detectors.

Simulations were done to explore the feasibility of the DARING technique. As an example, we simulated the trapping of an arbitrary ion of mass 250, its α decay at a random time inside the trap, the trajectory of the α particle and recoil, and finally the emission and trajectories of two electrons. The energies of the α particle and electrons were chosen to be 6 MeV, 100 eV and 2 keV, respectively. The time between the emission of the electrons was randomly chosen with a half life of 200 ps. We used a detector position resolution of 0.1 mm as specified for the RoentDek MCP delay line [24]. The reconstructed decay time for 2000 ions is shown in Fig. 3. Many sources of error can affect the estimation of the lifetime, the most important of which is the curvature
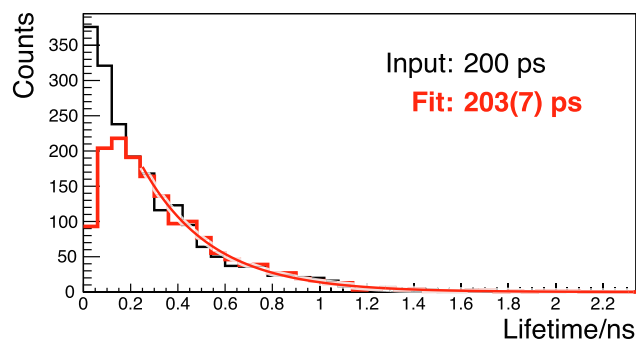

Fig. 3. Generated (black) and measured (bold red) values of the lifetime of an arbitrary state of half-life 200 ps. The "Fit" value of 203(7) ps corresponds to a simple exponential fit of the measured distribution. (For interpretation of the references to colour in this figure legend, the reader is referred to the web version of this article.)

radius of the electrons. If an electron is emitted along a field line (i.e. polar angle $\theta = 0$) it will follow this field line up to the detector. Otherwise the electron will follow a corkscrew trajectory crossing once per revolution the field line passing by its emission point. Thus, the detection point is usually not precisely the image of the emission point. If the electrons are emitted too close to each other, as in Fig. 4, their detection points may be scrambled. Since these points are used to determine the azimuthal angle of the α/recoil trajectories, errors on the detection points can lead to impossible scenarios in which the calculated direction of the α-particle is not compatible with its actual
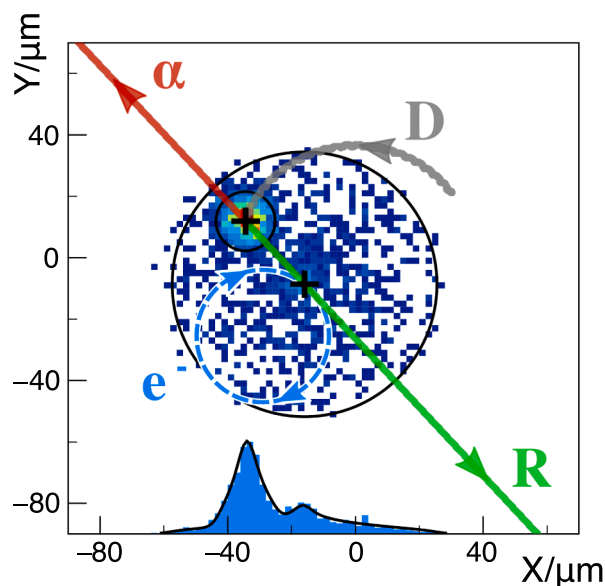

Fig. 4. Short decay event. This figure shows the trajectories of a decaying mother nucleus (grey **D**), its recoiling daughter nucleus (green **R**) and the outgoing α-particle (red α) in the XY-plane, as well as the positions of electron emission (black crosses). Population and decay of the excited state of the daughter nucleus are separated by 100 ps. The superimposed 2D histogram shows a typical distribution of reconstructed electron positions, the error coming from the detector's resolution and the curvature radius of each electron. The thin black circles are the theoretical boundaries of the two distributions. The distribution corresponding to the decay is larger than the one corresponding to the population due to the higher electron energy. These distributions have been described in [26] and their X-projection (bottom) agrees remarkably well with the theoretical expectation. The blue dashed circle shows the trajectory of a hypothetical electron emitted at close to 90° from the beam axis, thus having the maximum curvature radius at its energy. (For interpretation of the references to colour in this figure legend, the reader is referred to the web version of this article.)

detection point in the SSDs. The event is ignored in such a case, which explains the loss of statistics at short decay times in Fig. 3. This simple simulation confirms the feasibility of the method, but to estimate its true limits requires a more realistic electron distribution following α decay, as was done for ^{219,220}Rn in [25].

6. Future work and perspectives

Simulations concur in the feasibility of the DARING method with a MCP. A further interest of using a MCP to detect electrons is that the added information of the electron time-of-flight can be used to estimate the uncertainty of the electron detection position and thus deduce the emission point more accurately. This approach is being explored to increase the fraction of usable statistics for lifetime measurements and will be detailed in a forthcoming publication. Other simulations are being done to test the compatibility of the detector trap with precision mass measurements which indicate that its performances could be on par with cylindrical traps. The mechanical design has been completed and tests of the silicon detectors with an α source outside the magnetic field will take place early 2019. The first offline test of the spectroscopic assembly could use a pellet of ^{223}Ra, one of the only α emitters with a half-life long enough (11.4 d) to create a source but whose daughter nuclei ^{219}Rn has a half-life short enough to decay in the trap (3.96 s). Regarding online commissioning at ALTO, a feasible case has been identified: ^{196}Po can be produced via the ^{172}Yb(^{28}Si,4n)^{196}Po fusion-evaporation reaction. It has a half-life of 5.8 s and populates a 0^+ state in the daughter nuclei ^{192}Pb. The half-life of this state is not well known (0.75(10) ns), making this nucleus an ideal test subject to investigate the capabilities of the recoil distance method.

Acknowledgements

References

[1] E. Minaya Ramirez, et al., Nucl. Instr. Meth. B, this issue.
[2] B. Blank, et al., Int. J. Mass Spectrom. 349–350 (2013) 264–269, https://doi.org/10.1016/j.ijms.2013.03.006 100 years of Mass Spectrometry.
[3] V. Kolhinen, et al., Nucl. Instr. Meth. A 600 (2) (2009) 391–397, https://doi.org/10.1016/j.nima.2008.12.004.
[4] M. Block, et al., Eur. Phys. J. D 45 (2007) 39–45, https://doi.org/10.1140/epjd/e2007-00189-2.
[5] S. Kreim, et al., Nucl. Instr. Meth. B 317 (2013) 492–500, https://doi.org/10.1016/j.nimb.2013.07.072 XVIth International Conference on ElectroMagnetic Isotope Separators and Techniques Related to their Applications.
[6] T. Eronen, et al., Eur. Phys. J. A 48 (2012) 46, https://doi.org/10.1140/epja/i2012-12046-1.
[7] J. Ketelaer, et al., Phys. Rev. C 84 (2011) 014311, https://doi.org/10.1103/PhysRevC.84.014311.
[8] E. Minaya Ramirez, et al., Nucl. Instr. Meth. B 376 (2016) 298–301, https://doi.org/10.1016/j.nimb.2016.01.044 Proceedings of the XVIIth International Conference on Electromagnetic Isotope Separators and Related Topics.
[9] W. Huang, et al., Nucl. Instr. Meth. B 317 (2013) 528–531, https://doi.org/10.1016/j.nimb.2013.07.041 XVIth International Conference on ElectroMagnetic Isotope Separators and Techniques Related to their Applications.
[10] G. Savard, et al., Phys. Lett. A 158 (5) (1991) 247–252, https://doi.org/10.1016/0375-9601(91)91008-2.
[11] M. König, et al., Int. J. Mass Spectrom. 142 (1) (1995) 95–116, https://doi.org/10.1016/0168-1176(95)04146-C.
[12] S. Eliseev, et al., Phys. Rev. Lett. 110 (2013) 082501, https://doi.org/10.1103/PhysRevLett.110.082501.
[13] C. Weber, et al., Hyperfine Interact. 227 (1) (2014) 247–258, https://doi.org/10.1007/s10751-014-1044-5.
[14] C. Weber, et al., Nucl. Instr. Meth. B 317 (2013) 532–536, https://doi.org/10.1016/j.nimb.2013.07.048 XVIth International Conference on ElectroMagnetic Isotope Separators and Techniques Related to their Applications.
[15] C. Weber, et al., Int. J. Mass Spectrom. 349–350 (2013) 270–276, https://doi.org/10.1016/j.ijms.2013.05.006 100 years of Mass Spectrometry.
[16] L. Weissman, et al., Nucl. Instr. Meth. A 492 (3) (2002) 451–463, https://doi.org/10.1016/S0168-9002(02)01368-2.
[17] S. Rinta-Antila, et al., Hyperfine Interact. 223 (1) (2014) 73–80, https://doi.org/10.1007/s10751-012-0606-7.
[18] M. Mehlman, et al., Nucl. Instr. Meth. A 712 (2013) 9–14, https://doi.org/10.1016/j.nima.2013.02.004.
[19] A. Lennarz, et al., Phys. Rev. Lett. 113 (2014) 082502, https://doi.org/10.1103/PhysRevLett.113.082502.
[20] K. Leach, et al., Nucl. Instr. Meth. A 780 (2015) 91–99, https://doi.org/10.1016/j.nima.2014.12.118.
[21] J.-M. Régis, et al., Nucl. Instr. Meth. A 726 (2013) 191–202, https://doi.org/10.1016/j.nima.2013.05.126.
[22] A. Dewald, et al., Prog. Part. Nucl. Phys. 67 (2012) 786–839, https://doi.org/10.1016/j.ppnp.2012.03.003.
[23] D. Dahl, Int. J. Mass Spectrom. 200 (1) (2000) 3–25.
[24] Roentdek products manuals. URL:http://roentdek.com/manuals.
[25] N. Wandkowsky, et al., New J. Phys. 15 (8) (2013) 083040, https://doi.org/10.1088/1367-2630/15/8/083040.
[26] P. Kruit, F.H. Read, J. Phys. E Sci. Instrum. 16 (1983) 313–324, https://doi.org/10.1088/0022-3735/16/4/016.